 https://doi.org/10.3311/PPci.19612

Periodica Polytechnica Civil Engineering, 66(3), pp. 798–808, 2022

Experimental Study on the Effect of Fibers on Engineered Cementitious Composite Short Square Columns

Mohsen Dayyani[1], Alireza Mortezaei[2*], Mohammad Sadegh Rouhanimanesh[1], Jafar Asgari Marnani[1]

[1] Central Tehran Branch, Islamic Azad University, Punak Square, Chahar Bagh Blvd., 1955847881 Tehran, Iran
[2] Seismic Geotechnical and High Performance Concrete Research Centre, Department of Civil Engineering, Semnan Branch, Islamic Azad University, Damqan Road, 35135-179 Semnan, Iran
[*] Corresponding author, e-mail: a.mortezaei@semnaniau.ac.ir

Received: 30 November 2021, Accepted: 08 March 2022, Published online: 04 May 2022

Abstract

Recent earthquakes severely damaged short columns due to high lateral stiffness and low ductility. Some conditions, such as reductions in the heights of some columns compared to others on the same floor, deep beams, partially buried basements, and non-structural walls, cause short column effects. The prominent characteristics of engineered cementitious composites (ECCs) reinforced with polyvinyl alcohol (PVA) fibers – including their high tensile strength, micro and multiple cracks, energy dissipation, high ductility, and strain hardening – lead to improved seismic performance and economic efficiency in structure elements. In this study, 11 ECC columns with different fiber fractions (0–1.5%) and aspect ratios (3–7), as well as one conventional concrete column, were tested and evaluated. The results showed that increasing fiber friction and shear aspect ratio increased the length of the plastic hinge zone and ductility by at least 50% and 100%, respectively. Furthermore, the failure mode changed from brittle shear to ductile shear.

Keywords

PVA fibers, short columns, ECC, plastic joints

1 Introduction

In recent decades, research on conventional reinforced concrete frame structures has revealed that the short column conditions are a significant source of severe earthquake damage. Intense seismic excitation affects reinforced concrete columns and bridge piers as the main load-bearing structural members [1–3]. Column failure during earthquakes severely damages the entire structure and can cause destruction, casualties, financial losses, and mortality.

Therefore, the safe design of columns has been the subject of research in recent years. Reductions in the column-free length the emergence of the short column phenomenon, and the increasingly frequent use of cementitious composites in the industry have encouraged researchers to investigate how to eliminate the shortcomings associated with these members, including their brittleness and non-ductility. For example, Li et al. [4–7] introduced engineered cementitious composites (ECCs), which are adequately resistant materials in terms of their ductility and tension, as an alternative to conventional concrete. ECCs are different from other types of high-strength cementitious materials, as they have a high ductility with a crack width limit of 100 μm and an ultimate tensile strain capacity of 5% [8].

As shown in Fig. 1, this type of concrete can withstand considerable tensile deformations and strain hardening; has desirable characteristics for structural components such as beams, columns, walls, and connections under the cyclic loads and fatigue; and is resistant to chloride attacks and sequential freezing and melting cycles due to their integrity [9].

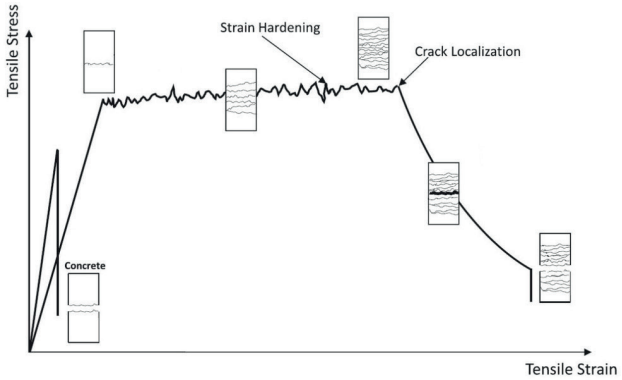

Fig. 1 A tensile stress-strain curve of an ECC

Cite this article as: Dayyani, M., Mortezaei, A., Rouhanimanesh, M. S., Marnani, J. A. " Experimental Study on the Effect of Fibers on Engineered Cementitious Composite Short Square Columns", Periodica Polytechnica Civil Engineering, 66(3), pp. 798–808, 2022. https://doi.org/10.3311/PPci.19612

Many studies have been conducted using ECCs as subsidiary material for the confinement, rehabilitation, and retrofitting of all or part of various concrete or masonry structural components [10–15]. In one such study conducted in 2003, Kawamata et al. [16] studied the behavior of the shear elements of ECCs under cyclic loads. As expected, the experiments showed that ECCs have higher energy dissipation than conventional concrete.

In other research, Parra-Montesinos and Wight [17] compared the behavior of beam-column connections containing conventional concrete and ECCs. They found that the hysteresis loops of the specimens made of ECCs were more stable and larger than conventional concrete-made columns while also showing less deterioration of resistance and a higher energy absorption capacity. In 2002, Fischer and Lee [18] examined failure in columns made of conventional reinforced concrete and those made of ECCs with no stirrups. They observed negligible crushing in ECC samples at large displacements and drifts, as well as increased spalling and rupture in conventional concrete samples at the supports. They also clearly demonstrated that ECCs have impressive strength under blast and seismic loads.

Kim et al. [19] examined the fatigue responses of the flexural components of ECCs in the bridge deck connections of actual scales. They found that cracks up to 0.6 mm continuously developed in conventional reinforced concrete until the end of the experiment, while the cracks observed in ECCs were limited to 50 μm. Kesner and Billington [20] studied the behavior of wall panels made of conventional concrete and ECCs, finding that ECCs performed better and exhibited higher maximum load-bearing and energy dissipation capacities under cyclic loads.

Walter et al. [21] performed an experiment on the decks of metal bridges and ECC beams under uniform flexural loads to investigate increases in stiffness and decreases in cracks caused by fatigue. The results showed that ECC beams were at least three times more resistant to the load than the other samples.

Despite the number of studies conducted on ECCS, a literature review suggests that few studies have examined structural ECC members and the seismic behavior and failure modes of ECC square columns. Furthermore, the few studies on this topic have mainly focused on ECCs as auxiliary materials for the confinement, rehabilitation, and strengthening of all or part of various concrete or masonry structural components.

Therefore, the present study was conducted to evaluate the seismic behavior of ECC square columns based on experimental results, including those related to displacement, absorption, energy dissipation capacity, failure modes, crack distribution, load-bearing capacity, ductility, the length of the yielding region, and other parameters affecting seismic behavior. The researchers demonstrated that ECCs' flexural members have two failure paths, which is similar to what the reinforced ECC tension stiffening members show under load [22]. The two failure paths were distinguished by forming single or dominant cracks, and the second path occurred via the gradual strain hardening of longitudinal reinforcing steel. The first failure path could not compensate for the load capacity by the hardening of longitudinal reinforcing steel, while the second failure path achieved a higher load capacity through the gradual strain hardening of longitudinal reinforcing steel [23–25].

Shakedown analyses were presented for perfectly plastic materials in 1932 and continued on indeterminate structures in 1938 [26, 27]. These analyzes focused on the elastic-plastic continuum [28]. Due to a lack of information about the magnitude of plastic deformations and residual displacements accumulated before the adaptation of the structure, Movahedi Rad [29, 30] suggested bounding theorems and approximate methods to determine the magnitude of the plastic deformations and residual displacements accumulated. Further, the mechanical models were introduced into the extended shakedown design [31]. The new type of plastic limit design procedures considers the influence of the limited load-carrying capacity of the beam-to-column connections of elasto-plastic steel frames under multi-parameter static loading and probabilistically given conditions [32]. The plastic hinge behavior and rotation capacity in reinforced ductile concrete flexural members were investigated using two-dimensional finite element models that could predict the equivalent plastic hinge length based on variables such as shear-span, tensile strength, reinforcement ratio, and the yield strength of the reinforcement [33]. The three-dimensional finite element method (FEM) on the behavior of plastic hinges in cyclically loaded RC columns showed all the lengths of the plastic hinge zones and revealed that the rebar yielding zone and curvature localization zone were significantly affected by loading types [34]. The researchers showed that the lengths of beams in the plastic hinge region were affected by the rebar yielding zone, concrete crushing zone, and curvature localization zone. The results show that none of the existing empirical models adequately predicts plastic hinge length [35].

2 Experimental program

2.1 Mix design and properties of ECCs

The ECC concrete matrix included 0–1.5% fiber fraction with high-tensile PVA fibers (as illustrated in Table 1 and Fig. 2), ordinary Portland cement, and fine aggregates (silica with a maximum grain size of 250 μm and a mean size of 110 μm). Table 2 shows the chemical requirements of Class F fly ash as designated in ASTM C618 [36], originating from anthracite and bituminous coal and mainly comprising alumina and silica.

The longitudinal reinforcements in the short columns comprised 10, 12, 16, 18, and 20 bars. The transverse reinforcements in the short columns and foundation beams also comprised hoops (10 mm in diameter). Table 3 and Fig. 3 present the tensile test results of the bars.

First, ECCs with five different fiber fractions (0–1.5%) and one conventional concrete specimen were designed.

Table 1 Properties of PVA fibers

Fiber name	RCS15
Manufacturer	Nycon
Color	yellowish white
Chemical stability	stable
Specific gravity	1300 kg/m^3
Length	8 mm
Configuration	Resin-bundled copped fiber

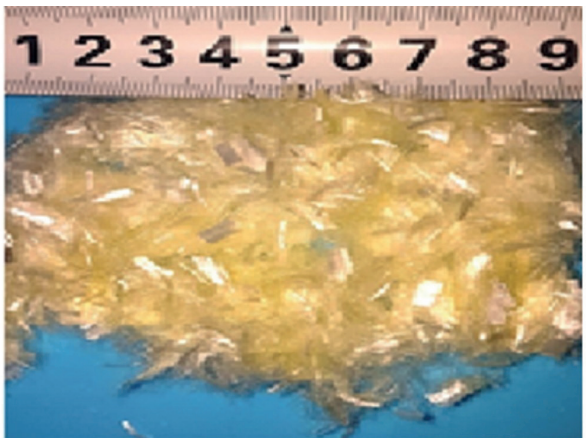

Fig. 2 RCS15 polymer fibers

Table 2 Chemical composition of Class F fly ash

Property	ASTM C618 Requirements (%)
SIO_2+Al_2O_3+Fe_2O_3	70
SO_3	5
Moisture content	3
Loss on ignition	6

Table 3 Tensile test results of the bars

Diameter (mm)	Area (mm)	Yield Strength (MPa)	Ultimate Strength (MPa)
10	78.5	475	510
12	113.04	463	542
16	419	419	495
18	665	465	545
20	406	406	471

Fig. 3 Tensile test of reinforcing bars

Six samples were tailored to verify the compression strength of ECC admixtures, as well as some other parameters. Finally, 12 cubic compression specimens (six bending specimens and six Brazilian splitting tensile specimens) were tested; and several cubic specimens with dimensions of 100 × 100 × 100 mm prepared with concrete and ECCs were tested under compression. The reinforced ECC specimens were tested on day 28 ± 2 days.

The difference between the estimated compressive strengths of the concrete and ECC specimens was reduced by allowing the reinforced concrete specimen to cure longer – these samples were tested on day 56 ± 2 days. The compressive strength of the concrete and ECC specimens were 35.40 and 38.56 MPa, respectively. Fig. 4 depicted the sample test. Table 4 and Fig. 4 represent the ECC sample test and ECC mix design by weight, respectively.

The density of the concrete used was 1900 kg/m^3, and its water-to-cement ratio was 0.63. The standard mix sequence was adjusted to increase viscosity and improve fiber dispersion. The deformation of fresh ECCs was investigated on-site to ensure proper self-consolidation behavior. Fig. 5 shows the sequence of on-site material charging.

Fig. 4 The ECC sample test

Table 4 ECC mix design by weight

Cement	Fly Ash	Sand	Water	HRWR*	Fiber (%)
1	1.2	0.8	0.63	0.012	0–1.5%

*High Range Water Reducer

Fig. 5 Sequence of on-site material charging

2.2 Preparing the specimens

This study tested several column specimens to investigate the seismic behaviors of reinforced concrete and ECC short columns with different aspect ratios and fiber percentages (Table 5).

The ECC material was cast into the connection part of the foundation beam to avoid weakening the interface between the column and foundation beam (Fig. 6).

Moreover, Table 5 and Fig. 7 present the specimens' details and layout, respectively. The 12 reinforcement concrete specimens were moist cured for seven days and allowed to cure at room temperature until testing. Longitudinal bars and transverse bars were monitored with six and three strain gages, respectively, with 0.15H*, 0.20H*, and 0.45H*, H* representing the height of the column. Seven concrete strain gages were affixed on concrete specimens (Fig. 6).

2.3 Test equipment and loading procedure

As illustrated in Fig. 8, loading conditions were established by fixing the bottom stub of each specimen to the base. This loading configuration was selected to promote flexural deformation in all specimens and investigate the effect of the ECC material on the expected plastic hinge region. Lateral loads were applied using a reaction wall equipped with a 250-kN actuator following a predetermined displacement-controlled loading sequence. Fig. 9 illustrates the cyclic lateral loads applied to the specimens [37].

3 Experimental results

3.1 Failure mechanism

During strong earthquakes, plastic deformation is localized to a small area. The performance of the plastic hinge zone is critical, as it governs the load carrying and deformation capacities of the member. In this zone, longitudinal steel yields, and the concrete is severely cracked and spalled. Park and Paulai [37] and Mortezaei [38] and Mortezaei and Mothagi [39] expressed the total displacement of columns in terms of curvature, column height,

Table 5 Geometry and reinforcement of the column specimens

Specimen	Material	Cross section	Height (mm)	Aspect ratio	Fiber (%)	Longitudinal bars	Transverse bars
SP1	ECC	250 × 250	750	3	0	8Φ10	5Φ10
SP2	ECC	300 × 300	900	3	0	8Φ12	5Φ10
SP3	ECC	350 × 350	1050	3	0.3	14Φ12	6Φ10
SP4	ECC	400 × 400	1200	3	0.3	16Φ12	6Φ10
SP5	RC	400 × 400	1200	3	0.0	16Φ12	6Φ10
SP6	ECC	200 × 200	1000	5	0.6	8Φ10	7Φ10
SP7	ECC	250 × 250	1250	5	0.6	8Φ12	8Φ10
SP8	ECC	350 × 350	1750	5	0.6	8Φ18	10Φ10
SP9	ECC	300 × 300	1800	6	1.0	8Φ16	10Φ10
SP10	ECC	350 × 350	2100	6	1.5	8Φ20	10Φ10
SP11	ECC	200 × 200	1400	7	1.0	8Φ10	10Φ10
SP12	ECC	250 × 250	1750	7	1.5	8Φ16	10Φ10

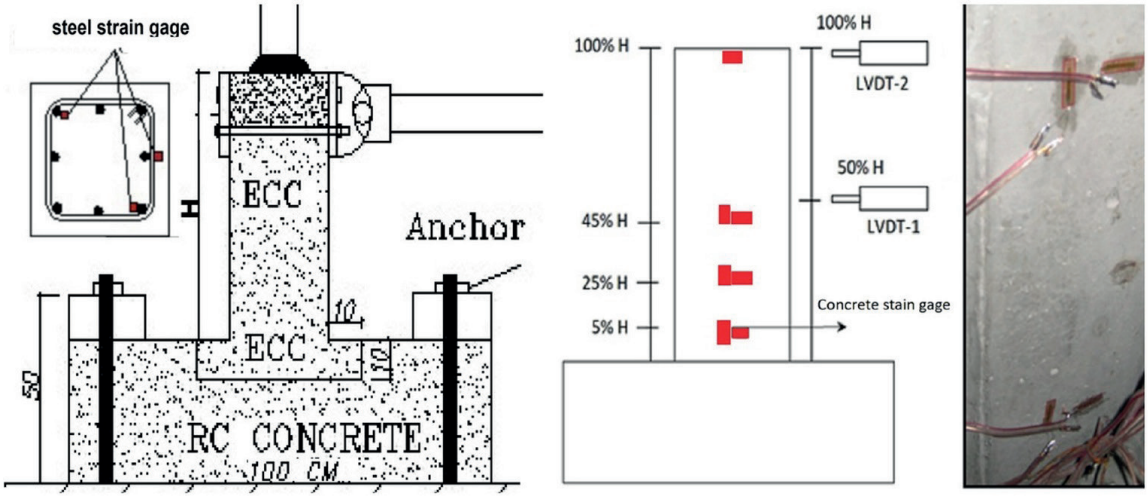

Fig. 6 Manufacturing process of the column specimens

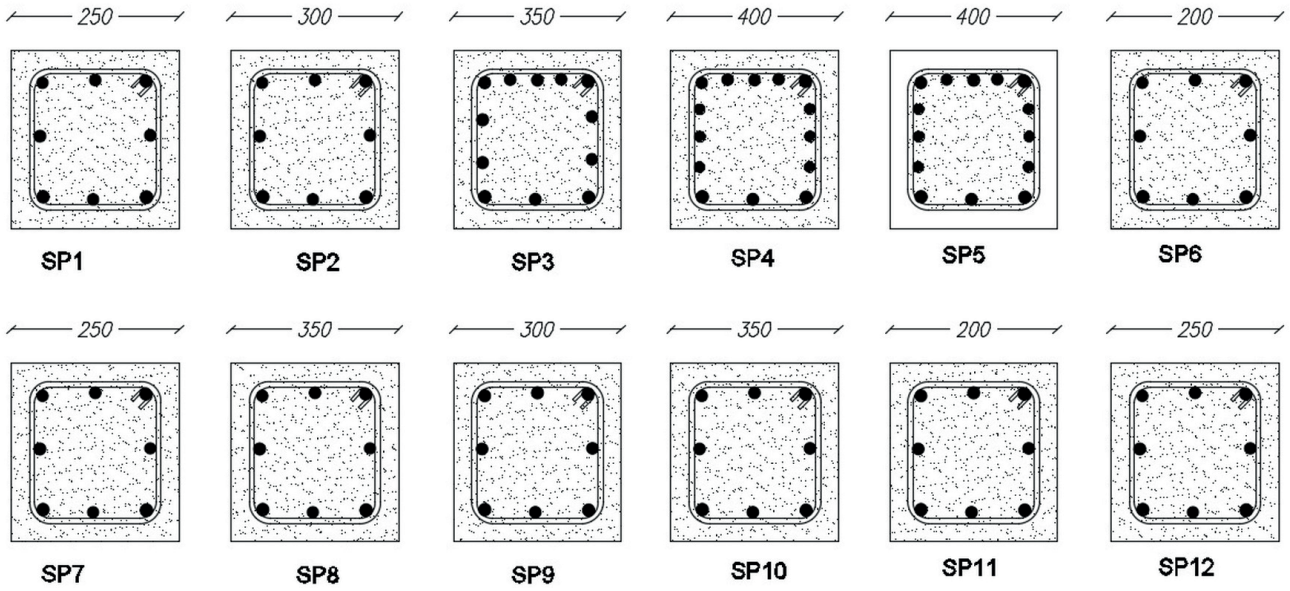

Fig. 7 Column reinforcement layouts

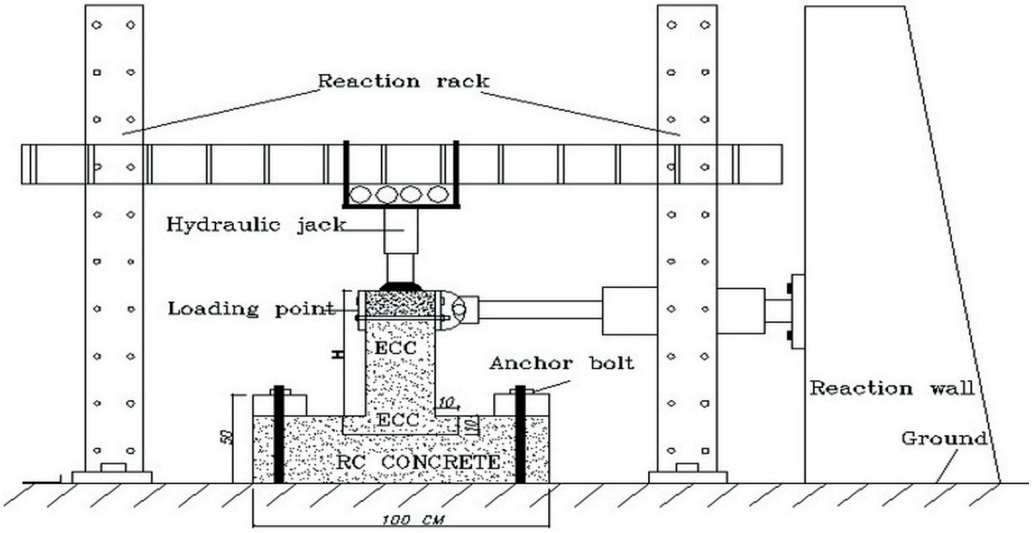

Fig. 8 Test setup of the specimens

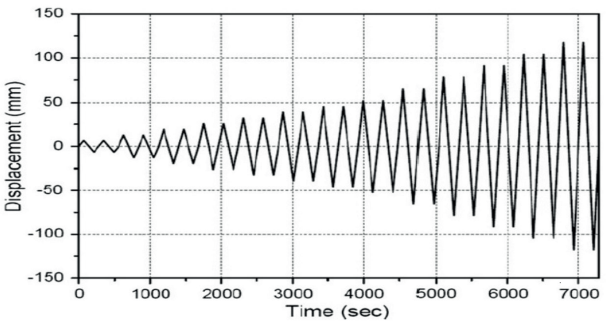

Fig. 9 Displacement-controlled cyclic lateral loads

and yield zone length. Since plastic hinge length is difficult to estimate using computer programs, it is often estimated based on experimental data using empirical equations. The length of the plastic hinge is affected by various factors, such as shear stress, the compressive strength of the concrete, moment gradient, and axial load. This study examined the effects of the fiber content and aspect ratio.

Fig. 10 presents the cracking patterns observed in the specimens. There were many similarities between the three specimens without fiber fractions (i.e., Sp1, Sp2, and Sp3).

Fig. 10 Cracking patterns of the specimens after failure

When the dominant cracks formed, specimens underwent material softening and failed due to the decreased tension stress.

Increasing the external load caused diagonal cracks to spread at the base of the column in the fiber-free specimens (i.e., S1, S2, and S5). It also caused concrete failure through severe spalling in cover and concrete materials. Shear cracks also exposed stirrups and longitudinal reinforcements at the base of the columns. The longitudinal bar yielded, and localized cracks occurred at 410 mm and 250 mm from the bottom of the ECC (SP4) and conventional concrete (SP5) specimens, respectively. Yielding was not observed in the transverse bar of the ECC column in this region. Fig. 11 shows the final cracking patterns of SP4 and SP5.In some specimens (Sp4, Sp6, Sp7, Sp8, Sp9, Sp10, Sp11, and Sp12), cracking manifested as horizontal flexural cracks with no diagonal (shear) cracks due to the inherent shear strength provided by the ECC composite itself.

Fiber bridging increases stress until a second crack forms at the location of the next weakest plane in the matrix. Fiber bridging across the micro-crack width in the reinforced ECC specimens facilitated strain accumulation in the reinforcing bars; thus, steel's plasticity contributed to more energy dissipation in ECC specimens than in conventional concrete specimens. In Sp1, Sp2, and Sp3, the width and length of splitting cracks increased.

S3-S4 and S6-S12 failed in their flexural mode, with multiple fine cracks distributed away from the base of the column. Also, increasing the fiber fraction and aspect ratio improved the plastic hinge zone. Shear cracking and buckling were observed 0.2–1.0 D* from the column base in longitudinal reinforcing bars in SP5 (D* is the dimension of column).

Table 6 presents the load characteristics, including crack load P_{cr}, yield load P_y, peak load P_{cr}, and ultimate load P_u, along with their corresponding displacements obtained from the hysteretic loops of the specimens. Moreover, $\theta_u = \Delta_u/H$ was used to evaluate ductility and deformation capacity.

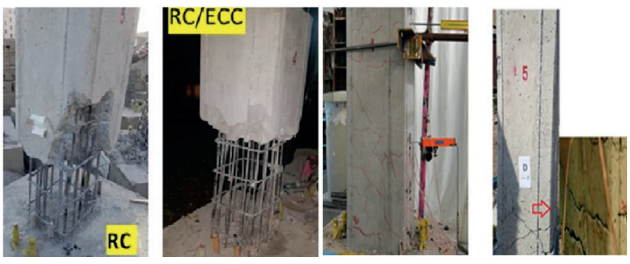

Fig. 11 Failure patterns of SP4 and SP5

Table 6 Displacement values and ductility coefficients of specimens

Specimen	S4	S5
P_{cr} (kN)	69.84	37.44
Δ_{Cr} (mm)	8.17	7.41
P_y (kN)	159.08	85.28
Δ_y (mm)	22.36	30.03
P_m (kN)	194	104
Δ_m (mm)	43	39
Δ_u (mm)	54.90	48.36
$\theta_u = \Delta_u/H$	0.0645	0.0403
$\mu = \Delta_u/\Delta_y$	2.46	1.61

3.2 Hysteresis loops

Hysteresis loops express cyclic loads in terms of lateral displacement. Fig. 12 shows the hysteresis loops of S4 and S5, for which the hysteresis loops showed noticeable pinching effects, suggesting more brittle failure and less energy absorption in the conventional concrete specimen than S4. The shear cracks that developed in S5 during the loading process rapidly decreased the lateral stiffness of the specimen and significantly intensified the pinching effect. The stability of S4 was significantly higher than that of S5, and its hysteresis loops were more complete.

The greater number of hysteretic loops maintained under cyclic loads in S4 (and their smaller and narrower areas before cracking) suggest that the columns remained in the elastic stage. The higher pick load and plastic deformation capacity of SP4 also suggest that the failure mode of the ECC short column can change from brittle flexure-shear failure to ductile flexural failure.

In Sp1, Sp2, and Sp3, crushing was observed upon the first negative excursion (7%) and eventually led to abrupt failure. During the first positive excursion (10%), Sp5 developed a major diagonal crack in the plastic hinge region, which led to lateral translation, cover spalling, and the debonding of concrete from the steel reinforcement.

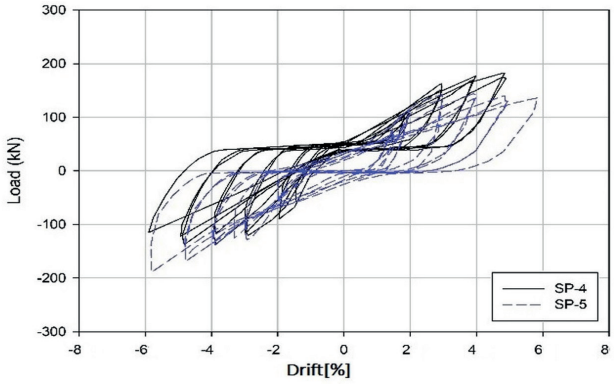

Fig. 12 Hysteresis loops of SP4 and SP5

Fig. 13 The hysteresis curves of the test specimens

Fig. 13 shows the hysteresis responses of the 12 specimens listed in Table 5. The cracks observed in the ECC columns were fine and more horizontal (indicating flexural strength) than those observed in the conventional concrete specimen. Spalling was also more prominent in the reinforced concrete specimens than in the reinforced ECC columns owing to the fibers in the ECC columns. The fine cracks in the ECC specimens facilitated better bonding to the fiber reinforcement than in the reinforced concrete specimens.

The increased bond toughness of the ECC columns also led to more rapid strain accumulation. Strain was higher in the steel reinforcements of the ECC specimens than in the concrete specimens. Moreover, the pinching of the hysteresis loops was more pronounced in the reinforced concrete than in reinforced ECC specimens. ECC columns underwent strain compatibility beyond yield, whereas SP5 did not.

Strain in the steel reinforcements was localized and accumulated differently between specimens of different materials, as well as in different sections. Fig. 14 shows the first yielding recorded displacements of the specimens observed when longitudinal reinforcement yielding began. More fine cracks and cases of plastic deformation were observed in the reinforced ECC specimens than in the conventional concrete specimens, which led to a difference in the amount of normalized energy dissipated per cycle.

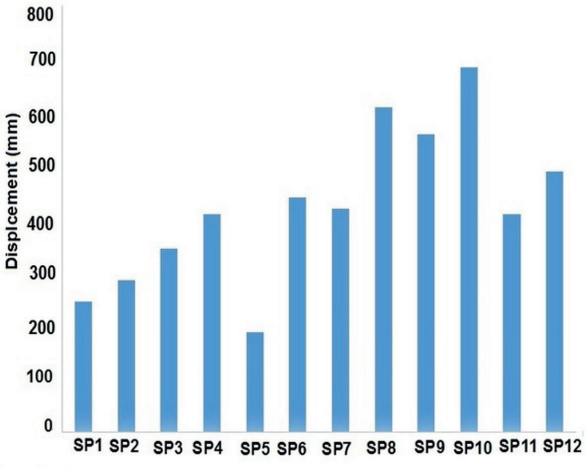

Fig. 14 Yielding displacement of longitudinal reinforcement

The strain gages installed on transverse bars did not exceed the yield strain. The length of the plastic hinge is summarized in Table 7 based on the strain gage data, which is used to monitor the strain of longitudinal bars and the surfaces of specimens. The test showed that the length of the plastic hinge doubled after increasing the aspect ratio and fiber fraction. The distribution of micro-cracks in SP12, SP11, SP10, and SP9 was higher than in SP7, SP6, and SP4.

4 Conclusions

In this study, 11 ECC columns with different fiber fractions (0–1.5%) and aspect ratios (3–7), as well as one conventional concrete column, were tested and evaluated. The main findings of this research are as follows:

1. Increasing the aspect ratio from 3–7 and the fiber percentage from 0%–1.5% caused the plastic hinge zone of ECC specimens to reach twice that of the conventional concrete specimen with the same geometry and reinforcing bars ratio.
2. Due to the micromechanical properties of ECCs and fiber bridging, the plastic joints of ECC specimens were twice as long as those of the ordinary concrete specimen with the same geometry and rebar ratio.
3. According to the strain-gage data, which was used to monitor transverse bars, the strains remained in the elastic state, which indicates the desirable performance of ECC specimens.
4. Reinforced ECC specimens dissipated more energy than reinforced concrete specimens. They also exhibited more ultimate drift and resistance to splitting and spalling with the same amount of transverse steel reinforcement.

The ECC columns continued to carry loads beyond yielding due to strain hardening and fiber-bridging, whereas the conventional concrete specimen did not.

Table 7 Length of the plastic hinge

Aspect ratio	Fiber fraction	Length of the plastic hinge
3	0–0.3%	1.0 D*
5	0.6%	1.5 D*
7	1–1.5%	2D*

D* represents the dimension of column

References

[1] Yi, W.-J., Zhou, Y., Hwang, H.-J., Cheng, Z.-J., Hu, X. "Cyclic loading test for circular reinforced concrete columns subjected to near-fault ground motion", Soil Dynamics and Earthquake Engineering, 112, pp. 8–17, 2018. https://doi.org/10.1016/j.soildyn.2018.04.026

[2] Chae, Y., Lee, J., Park, M., Kim, C.-Y. "Fast and slow cyclic tests for reinforced concrete columns with an improved axial force control", Journal of Structural Engineering, 145(6), 04019044, 2019. https://doi.org/10.1061/(ASCE)ST.1943-541X.0002334

[3] Huang, H., Hao, R., Zhang, W., Huang, M. "Experimental study on seismic performance of square RC columns subjected to combined loadings", Engineering Structures, 184, pp. 194–204, 2019. https://doi.org/10.1016/j.engstruct.2019.01.095

[4] Li, V. C. "Performance Driven Design of Fiber Reinforced Cementitious Composites", In: Swamy, R. N. (ed.) Proceedings of 4th RILEM International Symposium on Fiber Reinforced Concrete, E & FN Spon, London, UK, 1992, pp. 12–30. [online] Available at: http://hdl.handle.net/2027.42/84754

[5] Li, V. C. "Postcrack scaling relations for fiber reinforced cementitious composites", Journal of Materials in Civil Engineering, 4(1), pp. 41–57, 1992. https://doi.org/10.1061/(ASCE)0899-1561(1992)4:1(41)

[6] Li, V. C., Leung, C. K. Y. "Steady-state and multiple cracking of short random fiber composites", Journal of Engineering Mechanics, 118(11), pp. 2246–2264, 1992. https://doi.org/10.1061/(ASCE)0733-9399(1992)118:11(2246)

[7] Li,V. C., Wu, H.-C. "Conditions for pseudo strain-hardening in fiber reinforced brittle matrix composites", Applied Mechanics Reviews, 45(8), pp. 390–398, 1992. https://doi.org/10.1115/1.3119767

[8] Li, V. C., Wang, S., Wu, C. "Tensile strain-hardening behavior of polyvinyl alcohol engineered cementitious composite (PVA-ECC)", ACI Materials Journal, 98(6), pp. 483–492, 2001. [online] Available at: https://www.researchgate.net/publication/280229569

[9] Şahmaran, M., Lachemi, M., Li, V. C. "Assessing the durability of engineered cementitious composites under freezing and thawing cycles", Journal of ASTM International, 6(7), Paper ID: JAI102406, 2010. https://doi.org/10.1520/JAI102406

[10] Dehghani, A., Nateghi-Alahi, F., Fischer, G. "Engineered cementitious composites for strengthening masonry infilled reinforced concrete frames", Engineering Structures, 105, pp. 197–208, 2015. https://doi.org/10.1016/j.engstruct.2015.10.013

[11] Ebead, U., Shrestha, K. C., Afzal, M. S., El Refai, A., Nanni, A. "Effectiveness of fabric-reinforced cementitious matrix in strengthening reinforced concrete beams", Journal of Composites for Construction, 21(2), 04016084, 2017. https://doi.org/10.1061/(ASCE)CC.1943-5614.0000741

[12] Hung, C.-C., Chen, Y.-S. "Innovative ECC jacketing for retrofitting shear-deficient RC members", Construction and Building Materials, 111, pp. 408–418, 2016. https://doi.org/10.1016/j.conbuildmat.2016.02.077

[13] Al-Gemeel, A. N., Zhuge, Y. "Using textile reinforced engineered cementitious composite for concrete columns confinement", Composite Structures, 210, pp. 695–706, 2019. https://doi.org/10.1016/j.compstruct.2018.11.093

[14] Gao, S., Zhao, X., Qiao, J., Guo, Y., Hu, G. "Study on the bonding properties of Engineered Cementitious Composites (ECC) and existing concrete exposed to high temperature", Construction and Building Materials, 196, pp. 330–344, 2019. https://doi.org/10.1016/j.conbuildmat.2018.11.136

[15] Ge, W., Ashour, A. F., Cao, D., Lu, W., Gao, P., Yu, J., Ji, X., Cai, C. "Experimental study on flexural behavior of ECC-concrete composite beams reinforced with FRP bars", Composite Structures, 208, pp. 454–465, 2019. https://doi.org/10.1016/j.compstruct.2018.10.026

[16] Kawamata, A., Mihashi, H., Fukuyama, H. "Properties of hybrid fiber reinforced cement-based composites", Journal of Advanced Concrete Technology, 1(3), pp. 283–290, 2003. https://doi.org/10.3151/jact.1.283

[17] Parra-Montesinos, G., Wight, J. K. "Seismic response of exterior RC column-to-steel beam connections", Journal of Structural Engineering, 126(10), pp. 1113–1121, 2000. https://doi.org/10.1061/(ASCE)0733-9445(2000)126:10(1113)

[18] Fischer, G., Li, V. C. "Effect of matrix ductility on deformation behavior of steel-reinforced ECC flexural members under reversed cyclic loading conditions", Structural Journal, 99(6), pp. 781–790, 2002. https://doi.org/10.14359/12343

[19] Kim, Y. Y., Fischer, G., Li, V. C. "Performance of bridge deck link slabs designed with ductile engineered cementitious composite", Structural Journal, 101(6), pp. 792–801, 2004.

[20] Kesner, K., Billington, S. L. "Investigation of infill panels made from engineered cementitious composites for seismic strengthening and retrofit", Journal of Structural Engineering, 131(11), pp. 1712–1720, 2005. https://doi.org/10.1061/(ASCE)0733-9445(2005)131:11(1712)

[21] Walter, R., Li, V.C., Stang, H. "Comparison of FRC and ECC in a composite bridge deck", In: Proceedings of 5th PhD Symposium in Civil Engineering, Delft, The Netherlands, 2004, pp. 477–484. [online] Available at: http://hdl.handle.net/2027.42/84757

[22] Shao, Y., Billington, S. L. "Predicting the two predominant flexural failure paths of longitudinally reinforced high-performance fiber-reinforced cementitious composite structural members", Engineering Structures, 199, 109581, 2019. https://doi.org/10.1016/j.engstruct.2019.109581

[23] Bandelt, M. J., Billington, S. L. "Impact of reinforcement ratio and loading type on the deformation capacity of high-performance fiber-reinforced cementitious composites reinforced with mild steel", Journal of Structural Engineering, 142(10), 04016084, 2016. https://doi.org/10.1061/(ASCE)ST.1943-541X.0001562

[24] Frank, T. E., Lepech, M. D., Billington, S. L. "Experimental testing of reinforced concrete and reinforced ECC flexural members subjected to various cyclic deformation histories", Materials and Structures, 50(5), Article number: 232, 2017. https://doi.org/10.1617/s11527-017-1102-y

[25] Bleich, H. "Über die Bemessung statisch unbestimmter Stahltragwerke unter Berücksichtigung des elastisch-plastischen Verhaltens des Baustoffes" (On the design of statically indeterminate steel structures, taking into account the elastic-plastic behavior of the building material), Bauingenieur, 13, pp. 261–267, 1932. (in German)

[26] Melan, E. "Theorie statisch unbestimmter systeme (Theory of statically indeterminate systems)", In: International Association for Bridge and Structural Engineering, 2nd IABSE Congress, Berlin, Germany, 1936, pp. 43–64. (in German).
https://doi.org/10.5169/seals-2674

[27] Melan, E. "Zurplastizitat des raumlichen kontinuums (Plasticity of the spatial continuum)", Ingenieur-Archiv, 9, pp. 116–126, 1938. (in German)
https://doi.org/10.1007/BF02084409

[28] Rad, M. M. "A Review of Elasto-Plastic Shakedown Analysis with Limited Plastic Deformations and Displacements", Periodica Polytechnica Civil Engineering, 62(3), pp. 812–817, 2018.
https://doi.org/10.3311/PPci.11696

[29] Rad, M. M. "Optimal shakedown analysis of laterally loaded pile with limited residual strain energy", International Journal of Optimization in Civil Engineering, 8(3), pp. 347–355, 2018.

[30] Lógó, J., Movahedi Rad, M., Hjiaj, M. "Plastic Behaviour and Stability Constraints in the Reliability based Shakedown Analysis and Optimal Design of Skeletal Structures", In: Topping, B. H. V., Adam, J. M., Pallarés, F. J., Bru, R., Romero, M. L. (eds.) Proceedings of the Tenth International Conference on Computational Structures Technology, Civil-Comp Press, Stirlingshire, UK, 2010, Paper 203.
https://doi.org/10.4203/ccp.93.203

[31] Lógó, J., Rad, M. M., Knabel, J., Tauzowski, P. "Reliability based design of frames with limited residual strain energy capacity", Periodica Polytechnica Civil Engineering, 55(1), pp. 13–20, 2011.
https://doi.org/10.3311/pp.ci.2011-1.02

[32] Pokhrel, M., Bandelt, M. J. "Plastic hinge behavior and rotation capacity in reinforced ductile concrete flexural members", Engineering Structures, 200, 109699, 2019.
https://doi.org/10.1016/j.engstruct.2019.109699

[33] Yuan, F., Wu, Y.-F. "Effect of load cycling on plastic hinge length in RC columns", Engineering Structures, 147, pp. 90–102, 2017.
https://doi.org/10.1016/j.engstruct.2017.05.046

[34] Zhao, X.-M., Wu, Y.-F., Leung, A. Y. T. "Analyses of plastic hinge regions in reinforced concrete beams under monotonic loading", Engineering Structures, 34, pp. 466–482, 2012.
https://doi.org/10.1016/j.engstruct.2011.10.016

[35] ACI "Guide for testing reinforced concrete structural elements under slowly applied simulated seismic loads", American Concrete Institute, Farmington Hills, MI, USA, Rep. ACI 374.2R-13, 2013.

[36] ASTM "ASTM C618-19 Standard Specification for Coal Fly Ash and Raw or Calcined Natural Pozzolan for Use in Concrete", ASTM International, West Conshohocken, PA, USA, 2019.
https://doi.org/10.1520/C0618-19

[37] Park, R., Paulay, T. "Reinforced Concrete Structures", John Wiley & Sons, 1975. ISBN: 978-0-471-65917-4
https://doi.org/10.1002/9780470172834

[38] Mortezaei, A. "Plastic hinge length of RC columns under the combined effect of near-fault vertical and horizontal ground motions", Periodica Polytechnica Civil Engineering, 58(3), pp. 243–253, 2014.
https://doi.org/10.3311/PPci.7329

[39] Mortezaei, A., Motaghi, A. "Seismic assessment of the world's tallest pure-brick tower including soil-structure interaction", Journal of Performance of Constructed Facilities, 30(5), 04016020, 2016.
https://doi.org/10.1061/(ASCE)CF.1943-5509.0000861